Characterization of boron-doped micro- and nanocrystalline diamond films deposited by wafer-scale hot filament chemical vapor deposition for MEMS applications

Jingchun Zhang[1], Jerry W. Zimmer[2], Roger T. Howe[3], Roya Maboudian[1**]

[1]Department of Chemical Engineering, University of California, Berkeley, CA 94720

[2]sp3 Diamond Technologies, 2220 Martin Ave., Santa Clara, CA 95050

[3]Department of Electrical Engineering, Stanford University, Stanford, CA 94305

Abstract

Micro- and nanocrystalline diamond (MCD and NCD) films are deposited on 4 inch silicon substrates by a large area multi-wafer scale hot filament chemical vapor deposition (HFCVD) system. The films are in-situ doped by boron. The chemical and crystalline structures are studied by electron probe microanalysis (EPMA), Raman spectroscopy and X-ray diffraction (XRD). The microcrystalline films have a preferred (111) texture, while the nanocrystalline films exhibit (220) texture. Strain gauges and cantilever beam arrays are microfabricated by surface micro-machining technique to characterize the residual strain and strain gradient of the diamond films. Both micro- and nanocrystalline

**Corresponding author

films have small compressive strains of -0.052 % and -0.040 % respectively, with the strain gradient of 10^{-5} μm^{-1}. These values are low enough to enable the realization of many MEMS devices.

Introduction

The superior properties of diamond has made it an exceptional material for applications in harsh environments. Recently, advances in techniques for depositing diamond thin films on a variety of substrate materials have motivated increased studies for their applications in microelectromechanical systems (MEMS). [1, 2] Microwave plasma chemical vapor deposition (MPCVD) and hot filament chemical vapor deposition (HFCVD) are the mostly used processes to grow diamond thin films. While MPCVD offers more versatility in gas choice and process control, HFCVD is more attractive economically and easier to operate and maintain. In addition, HFCVD is currently capable of deposition on substrates of over twelve inches in diameter, which is far beyond the capability of the current MPCVD systems.

In this paper, we report on the characterization of diamond films deposited by a commercial HFCVD system capable of depositing on twelve inch substrate for MEMS applications. By varying the deposition conditions, microcrystalline diamond (MCD) and nanocrystalline diamond (NCD) are deposited. The morphology and properties of MCD and NCD films are fundamentally different due not only to their difference in grain sizes but also in the grain structure and electronic bonding characters. [3] As a material for MEMS structural layer, certain basic material properties of diamond films need to be characterized and optimized, including elastic modulus, fracture strength, residual strain and stress, electrical resistivity and surface morphology. In particular, proper residual strain is critical to ensure predictable behavior of micro-fabricated MEMS structures after they are released from substrates. However, characterization on

this issue is only reported recently for undoped diamond films. [4] In this paper, the residual strain properties of boron-doped MCD and NCD films deposited by HFCVD are characterized using a variety of microfabricated devices.

Experimental

Diamond films are deposited on 4 inch silicon wafers at 750 to 800 ℃ using CH_4 diluted in H_2 by a large area multi-wafer scale hot filament chemical vapor deposition system (Model 600, sp3 Inc.), which provides for uniform diamond growth over areas exceeding 350 mm by 375 mm. Varying CH_4/H_2 ratios and seeding processes are applied to grow MCD and NCD films. Boron vapor from solid source is introduced for in-situ p-type doping. *[growth pressure, rate and uniformity?]* Cameca SX-51 electron probe microanalysis (EPMA) is used for chemical composition analysis to determine the boron concentration. The diamond electronic bonding character is identified by Raman spectroscopy recorded by a Horiba spectrometer using a 633 nm Ar laser. The film surface topography is examined by a LEO 1550 high performance Schottky field emission scanning electron microscopy (SEM) and a DI Multimode III atomic force microscopy (AFM). X-ray diffraction (XRD) in θ-2θ mode obtained by a Siemens D5000 diffractometer is employed to analysis the crystalline orientation of the deposited films. The grain structure along the film thickness is studied by the cross-section SEM.

The residual strain and strain gradient along the film thickness are evaluated by microstrain gauges and cantilever beam arrays (CBA) respectively, which are fabricated by surface micromachining techniques. [5] The microfabrication flow is schematically illustrated in Fig. 1. The diamond film is patterned by a magnetically enhanced reactive ion etching system (Centura MxP+, Applied Materials Inc.) using O_2/CF_4 chemistry. SiO_2 is used as the etching mask which is deposited using SiH_4 and O_2 at 450℃ in a low pressure chemical vapor deposi-

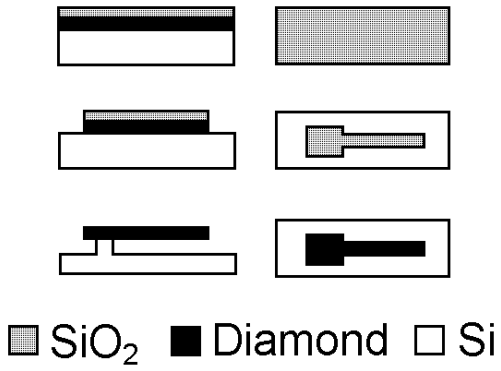

Figure 1: Schematic fabrication process flow for microstrain gauge and cantilever beam arrays.

tion (LPCVD) system and patterned by conventional photo-lithography. After patterning diamond film, the SiO_2 mask is removed using hydrogen fluoride solution. The diamond micro-structures are finally released by timed isotropic etching of the underlying silicon by gaseous XeF_2.

The microstrain gauge consists of two test beams (250 μm $\times$ 10 μm), one indicator beam (1000 μm $\times$ 10 μm), and two vernier gauges as show in Fig. 2. One end of the test beam is anchored to the substrate, and the other end is attached to the indicator beam. The two junctions of the test beams with the indicator beam are separated by a small distance (10 μm). After the test structure is released from the substrate, the residual strain in the film causes the deformation of the test beams. The small change in the length of the test beams are amplified at the ends of the indicator beam by its rotation. The displacement of the ends of the indicator beam (δ) can be read by SEM or an optical microscope and converted to the residual strain (ϵ) using Eq. 1:

$$\epsilon = \frac{\delta d}{L_i L_t} \tag{1}$$

where d is the distance between the junctions of the test beams with the indicator

beam, L_i and L_t are the length of indicator and test beams, respectively.

Figure 3 shows a CBA used to characterize the strain gradient. The cantilever beams are 50 μm to 1 mm long and 10 μm wide, and single-end anchored to the substrate. After release from the substrate, the strain gradient in the film causes the out of plane bending of the cantilever beams, which is measured by a Wyko NT3300 interferometer profiling system. For small deflections, and assuming that strain changes linearly through the film thickness, the strain gradient (γ) can be calculated using Eq. 2:

$$\gamma = \frac{2\Delta z}{L_c^2} \tag{2}$$

where Δz is the tip deflection and L_c is the length of the cantilever beam.

Results and Discussion

The Raman spectrum of boron doped MCD film (2.5 μm thick) shown in Fig. 4(a), features two sharp peaks at 1230 and 1318 cm^{-1}, and a broad weak peak around 1500-1600 cm^{-1}. The characteristic sp^3 diamond bonding peak is the zone-center phonon line located at 1332 cm^{-1}. [6] In our spectrum, this peak is down shifted to 1318 cm^{-1}. This shift is in accordance with the observation in previous Raman studies of boron doped diamond and is attributed to boron doping. [7] The peak at 1230 cm^{-1} is also a feature of boron incorporation in the diamond lattice and represents the combined peaks of single optical phonons. [8] It has been found the appearance of this peak is also related to laser source and it is absent in Raman spectrum obtained using higher energy excitation laser source. [9] The broad peak represents non-diamond phase including graphite and amorphous carbon. It is known that the Raman scattering cross section for graphite is 50 - 60 times higher than for diamond. The low intensity of this peak indicates the dominance of the sp^3 bonding in MCD films. In the case of NCD film (2.9 μm thick), aside for the peaks observed in the

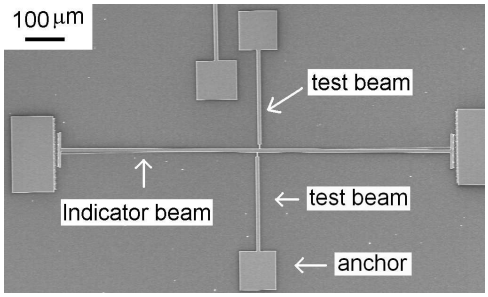

(a)

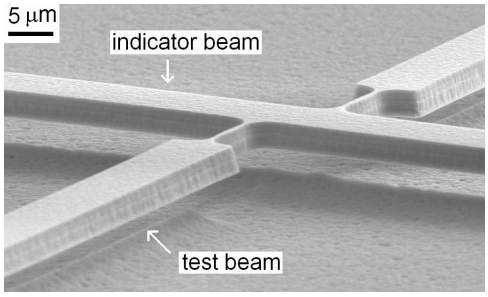

(b)

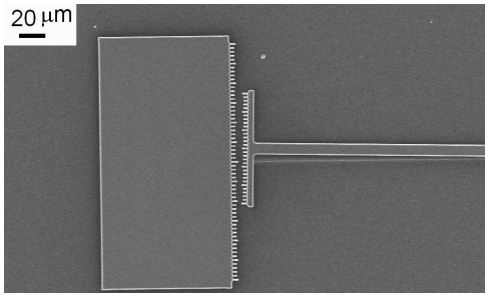

(c)

Figure 2: SEM images of microstrain gauge fabricated using doped NCD films: (a) full gauge, (b) junctions of two test beams with indicator beam and (c) vernier gauge.

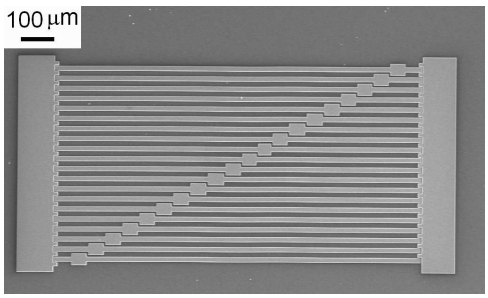

Figure 3: SEM image of cantilever beam array used to characterize the strain gradient.

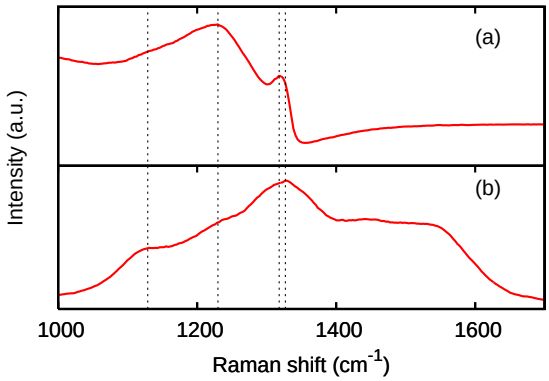

Figure 4: Raman spectra of boron doped (a) MCD and (b) NCD films.

spectrum of MCD, a peak at 1129 cm^{-1} is present (Fig. 4(b)). This peak is the well-known feature of nanocrystalline diamond arising from the sp^2 bonding at grain boundaries. The sp^3 diamond feature peak in NCD is at 1327 cm^{-1}, showing a relatively smaller down-shifting compared to that of MCD, and the characteristic boron doping peak at 1230 cm^{-1} is also weaker in NCD. This may imply lower boron incorporation in NCD films than that in MCD films under the same doping condition. The non-diamond peak is stronger in NCD than that in MCD; however, it is still weaker than the sp^3 peak, which implies the diamond phase is still dominant in the NCD films.

Figure 5 show the XRD spectrum of the boron doped MCD and NCD films. Beside the peaks from substrate, the MCD film shows solely (111) texture at $2\theta = 44.1°$, while the NCD film shows dominating (220) texture at $2\theta = 75.4°$ with small fraction of (111). The (111) and (220) peak positions correspond to lattice constants of 3.554 and 3.563 Å, which closely match that of diamond (3.567 Å). The sharp peaks in both MCD and NCD films indicate the high quality of diamond crystal. The difference in the preferred texture in the MCD and NCD films is related to the difference in CH_4/H_2 ratio used in the film growth. The (220) texture has been reported as a sign of high non-diamond incorporation, which agrees with the Raman spectrum presented in Fig. 4. [10]

The chemical composition analysis by EPMA shows the boron concentration in MCD and NCD films to be $(1.67 \pm 0.33) \times 10^{21}$ and $(1.50 \pm 0.30) \times 10^{21}$ cm^{-3} respectively. It has been reported that boron atoms prefer incorporation into the diamond growth along (111) orientation, hence a higher boron concentration may be expected in MCD films for the same boron doping conditions. [11] However, due to the overlap of boron peak and the long trail of carbon peak, it is beyond the capability of EPMA to discriminate the difference in boron concentration in the MCD and NCD films.

The SEM top view of the MCD film (Fig. 6(a)) shows a highly faceted surface. The grain size ranges from half to 1 μm with a root mean square (RMS) roughness of 71 nm measured by AFM. In contrast, the NCD film consists of fine spherical grains as small as 10 nm and has a smooth surface with an RMS of 20 nm. The grains in MCD have a wedge shape with increasing size from bottom to top, while the grains in NCD show uniform size along the film thickness as show in the cross-sectional SEM images in Fig. 7. Based on these analysis, the surface roughness of NCD film is expected to be independent on film thickness, while the surface of MCD film gets rougher with increasing thickness.

Based on the microfabricated strain gauges, both MCD and NCD films have small compressive residual strains of -0.052 ± 0.004 % and -0.040 ± 0.002 %

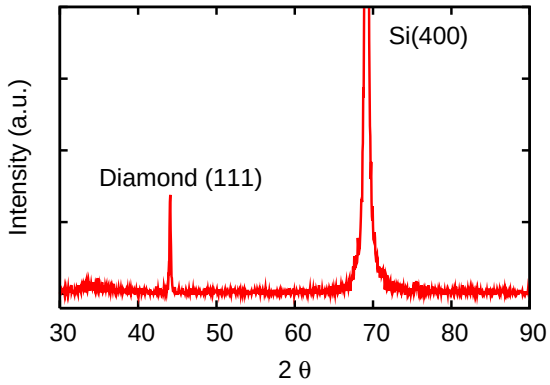

(a)

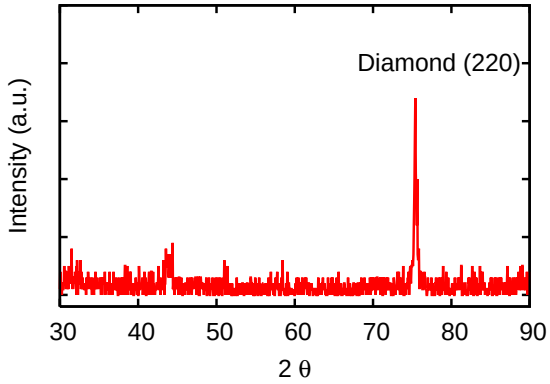

(b)

Figure 5: XRD spectra of boron doped (a) MCD and (b) NCD films.

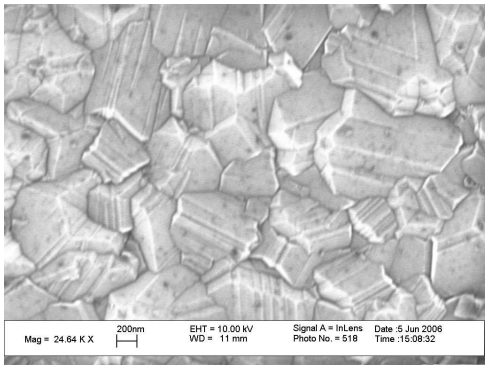

(a)

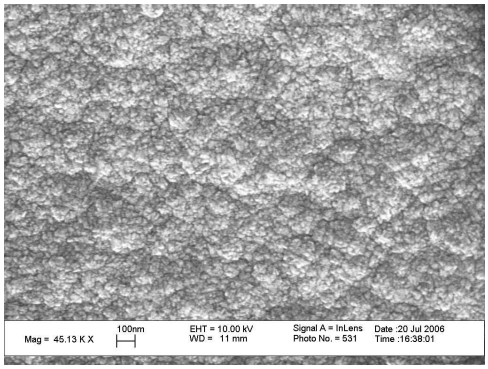

(b)

Figure 6: SEM top view images of (a) MCD and (b) NCD films.

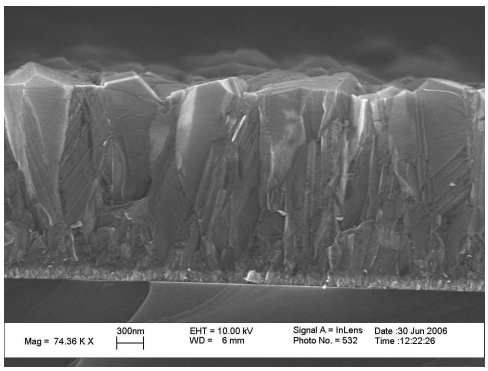

(a)

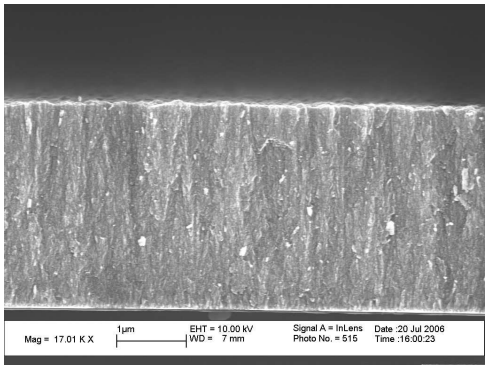

(b)

Figure 7: SEM cross-section view images of (a) MCD and (b) NCD films.

respectively. The residual strain is known to be composed of intrinsic strain and thermal strain. The thermal strain is caused by the mismatch in thermal expansion coefficients (TEC) between the film and the substrate, while the intrinsic strain is related to film microstructure. According to the TEC data of silicon and diamond in the temperature range of 300 to 1000 K, the thermal strain is estimated to be around -0.034 %. So the intrinsic strain in both MCD and NCD films are expected to be compressive. Based on the microfabricated cantilever beam arrays, the strain gradient of MCD and NCD are opposite in sign as shown in Fig. 8. The cantilevers made out of the MCD films bend up indicating a positive strain gradient of $(5 \pm 1) \times 10^{-5}$ μm^{-1}, while those made out of the NCD films bend down with a strain gradient of $(-3 \pm 1) \times 10^{-5}$ μm^{-1}. Both correspond to an out-of-plane bending around 1 μm or less for a 200 μm long cantilever beam. This is an acceptable value in many MEMS designs.

Conclusion

The microstructure and residual strain of boron doped microcrystalline and nanocrystalline diamond films deposited by large-scale hot filament chemical vapor deposition are studied. MCD and NCD films have preferred (111) and (220) texture respectively. The MCD film features increasing grain size with film thickness and a highly faceted surface, while the NCD film has uniform grain size and relatively smooth surface. The residual strain in both films are compressive. Both the residual strain and strain gradient of the MCD and NCD films are small enough to enable the realization of many MEMS devices.

Acknowledgments

...

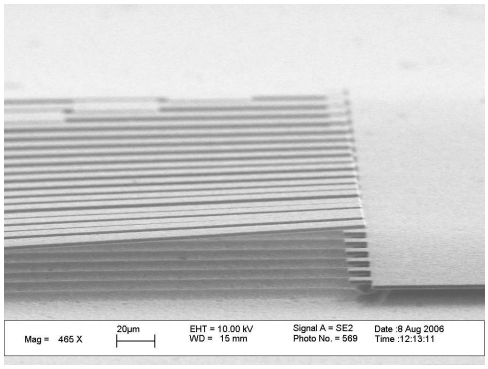

(a)

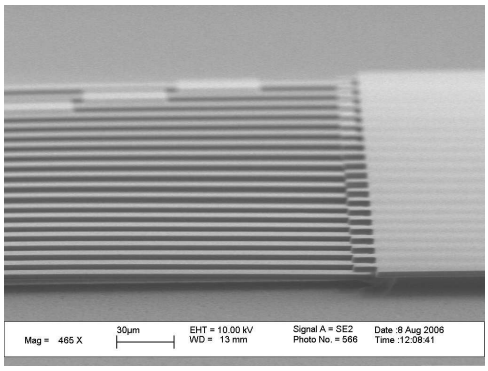

(b)

Figure 8: Cantilever beam array microfabricated from (a) MCD and (b) NCD films.

References

[1] E. Kohn, P. Gluche, M. Adamschik, Diamond MEMS a new emerging technology, Diamond and Related Materials 8 (2-5) (1999) 934–940.

[2] Y. X. Tang, D. M. Aslam, Technology of polycrystalline diamond thin films for microsystems applications, Journal of Vacuum Science & Technology B 23 (3) (2005) 1088–1095.

[3] T. Sharda, M. M. Rahaman, Y. Nukaya, T. Soga, T. Jimbo, M. Umeno, Structural and optical properties of diamond and nano-diamond films grown by microwave plasma chemical vapor deposition, DIAMOND AND RELATED MATERIALS 10 (3-7) (2001) 561–567.

[4] F. J. H. Guillen, K. Janischowsky, J. Kusterer, W. Ebert, E. Kohn, Mechanical characterization and stress engineering of nanocrystalline diamonds films for MEMS applications, Diamond and Related Materials 14 (3-7) (2005) 411–415.

[5] D. Gao, M. B. J. Wijesundara, C. Carraro, R. T. Howe, R. Maboudian, Characterization of residual strain in SiC films deposited using 1,3-disilabutane for MEMS applications, Journal of Microlithography, Microfabrication, and Microsystems 2 (2) (2003) 259–263.

[6] P. K. Bachmann, D. U. Wiechert, Optical characterization of diamond, Diamond and Related Materials 1 (5-6) (1992) 422–433.

[7] A. F. Azevedo, R. C. M. De Barros, S. H. P. Serrano, N. G. Ferreira, SEM and raman analysis of boron-doped diamond coating on spherical textured substrates, Surface and Coatings Technology 200 (20-21) (2006) 5973–5977.

[8] R. J. Zhang, S. T. Lee, Y. W. Lam, Characterization of heavily boron-doped diamond films, Diamond and Related Materials 5 (11) (1996) 1288–1294.

[9] R. Locher, J. Wagner, F. Fuchs, M. Maier, P. Gonon, P. Koidl, Optical and electrical characterization of boron-doped diamond films, Diamond and Related Materials 4 (5-6) (1995) 678–683.

[10] M. S. Haque, H. A. Naseem, A. P. Malshe, W. D. Brown, Study of stress in microwave plasma chemical vapor deposited diamond films using x-ray diffraction, CHEMICAL VAPOR DEPOSITION 3 (3) (1997) 129–135.

[11] P. Wurzinger, P. Pongratz, P. Hartmann, R. Haubner, B. Lux, Investigation of the boron incorporation in polycrystalline CVD diamond films by TEM, EELS and Raman spectroscopy, Diamond and Related Materials 6 (5-7) (1997) 763–768.